Circulation

ORIGINAL RESEARCH ARTICLE

A Rare Noncoding Enhancer Variant in *SCN5A* Contributes to the High Prevalence of Brugada Syndrome in Thailand

Roddy Walsh, PhD*; John Mauleekoonphairoj, PhD*; Isabella Mengarelli, PhD*; Fernanda M. Bosada, PhD; Arie O. Verkerk, PhD; Karel van Duijvenboden, PhD; Yong Poovorawan, MD; Wanwarang Wongcharoen, MD; Boosamas Sutjaporn, BNS; Pharawee Wandee, BSc; Nitinan Chimparlee, MD; Ronpichai Chokesuwattanaskul, MD; Kornkiat Vongpaisarnsin, MD; Piyawan Dangkao, BSc; Cheng-I Wu, MD; Rafik Tadros, MD, PhD; Ahmad S. Amin, MD, PhD; Krystien V.V. Lieve, MD, PhD; Pieter G. Postema, MD, PhD; Maarten Kooyman, MSc; Leander Beekman, BSc; Dujdao Sahasatas, MD; Montawatt Amnueypol, MD; Rungroj Krittayaphong, MD; Somchai Prechawat, MD; Alisara Anannab, MD; Pattarapong Makarawate, MD; Tachapong Ngarmukos, MD; Keerapa Phusanti, MD; Gumpanart Veerakul, MD; Zoya Kingsbury, BSc; Taksina Newington, PhD; Uma Maheswari, PhD; Mark T. Ross, DPhil; Andrew Grace, MBBS, PhD; Pier D. Lambiase, MBBS, PhD; Elijah R. Behr, MBBS, MD; Jean-Jacques Schott, PhD; Richard Redon, PhD; Julien Barc, PhD; Vincent M. Christoffels, PhD; Arthur A.M. Wilde, MD, PhD; Koonlawee Nademanee, MD*; Connie R. Bezzina, PhD*; Apichai Khongphatthanayothin, MD*

BACKGROUND: Brugada syndrome (BrS) is a cardiac arrhythmia disorder that causes sudden death in young adults. Rare genetic variants in the *SCN5A* gene encoding the $Na_v1.5$ sodium channel and common noncoding variants at this locus are robustly associated with the condition. BrS is particularly prevalent in Southeast Asia but the underlying ancestry-specific factors remain largely unknown.

METHODS: Genome sequencing of BrS probands and population-matched controls from Thailand was performed to identify rare noncoding variants at the *SCN5A-SCN10A* locus that were enriched in patients with BrS. A likely causal variant was prioritized by computational methods and introduced into human induced pluripotent stem cell (hiPSC) lines using CRISPR-Cas9. The effect of the variant on *SCN5A* expression and $Na_v1.5$ sodium channel current was then assessed in hiPSC-derived cardiomyocytes (hiPSC-CMs).

RESULTS: A rare noncoding variant in an *SCN5A* intronic enhancer region was highly enriched in patients with BrS (detected in 3.9% of cases with a case-control odds ratio of 45.2). The variant affects a nucleotide conserved across all mammalian species and predicted to disrupt a Mef2 transcription factor binding site. Heterozygous introduction of the enhancer variant in hiPSC-CMs caused significantly reduced *SCN5A* expression from the variant-containing allele and a 30% reduction in $Na_v1.5$-mediated sodium current density compared with isogenic controls, confirming its pathogenicity. Patients with the variant had severe phenotypes, with 89% experiencing cardiac arrest.

CONCLUSIONS: This is the first example of a functionally validated rare noncoding variant at the *SCN5A* locus and highlights how genome sequencing in understudied populations can identify novel disease mechanisms. The variant partly explains the increased prevalence of BrS in this region and enables the identification of at-risk variant carriers to reduce the burden of sudden cardiac death in Thailand.

Key Words: Asia, Southeastern ■ Brugada syndrome ■ genetics ■ noncoding genetic variant

Correspondence to: Roddy Walsh, PhD, Amsterdam UMC, Meibergdreef 9, 1105 AZ Amsterdam, The Netherlands. Email r.t.walsh@amsterdamumc.nl
*R. Walsh, J. Mauleekoonphairoj, I. Mengarelli, K. Nademanee, C.R. Bezzina, and A. Khongphatthanayothin contributed equally.
Supplemental Material is available at https://www.ahajournals.org/doi/suppl/10.1161/CIRCULATIONAHA.124.069041.
For Sources of Funding and Disclosures, see page 43.

Circulation is available at www.ahajournals.org/journal/circ

Clinical Perspective

What Is New?

- A rare genetic variant located in an *SCN5A* noncoding enhancer (RE5) was found to be highly enriched in patients with Brugada syndrome (BrS) from Thailand compared with population-matched controls.
- The variant disrupts a highly conserved nucleotide in a Mef2 transcription factor binding site and caused allele-specific reduction of *SCN5A* expression and a 30% decrease in sodium channel density in CRISPR-Cas9 edited human induced pluripotent stem cell–derived cardiomyocytes compared with isogenic controls.
- The RE5 variant is found in 4% of patients with BrS from Thailand and helps explain the high prevalence of the condition in Southeast Asia.

What Are the Clinical Implications?

- Although BrS is particularly prevalent in Southeast Asia, the yield of genetic testing in this population is much lower than in other regions, hindering the identification of at-risk individuals.
- By incorporating this variant into clinical genetic testing, the primary causal genetic factor will be detected in more affected families, enabling the diagnosis and clinical management of relatives that could prevent sudden cardiac deaths.
- This study demonstrates how rare noncoding variants, hitherto largely unexplored in cardiac genetic disease, can be discovered and validated and may facilitate the identification of additional variants at the *SCN5A* locus underlying the increased prevalence of BrS in East Asia.

Nonstandard Abbreviations and Acronyms

1KG	1000 Genomes
BrS	Brugada syndrome
GWAS	genome-wide association studies
hiPSC	human induced pluripotent stem cell
hiPSC-CM	human induced pluripotent stem cell–derived cardiomyocyte
OR	odds ratio
PCA	principal component analysis
RE	regulatory element
SNP	single nucleotide polymorphism
TF	transcription factor

Brugada syndrome (BrS) is a cardiac arrhythmia disorder associated with increased risk of sudden death in young adults and characterized by ST-segment elevation in the right precordial leads of the ECG, occurring either spontaneously or after challenge with sodium channel blockers (eg, ajmaline).[1] Rare loss-of-function coding variants in *SCN5A*, encoding the $Na_v1.5$ sodium channel underlying the cardiac sodium current (I_{Na}), are found in ≈20% of individuals of European ancestry with BrS.[2] Several other genes have been implicated in BrS but were considered to have limited evidence of association by ClinGen reevaluation, and *SCN5A* remains the only clinically actionable gene.[3,4] Genome-wide association studies (GWAS) have demonstrated a strong contribution of common genetic variation to BrS susceptibility (single nucleotide polymorphism [SNP]–based heritability, $h2_{SNP}$, between 0.17 and 0.34), indicating the genetic architecture is more complex than a simple monogenic disease model.[5]

Eight of the 21 independent genome-wide significance signals detected by the BrS GWAS were located at the *SCN5A–SCN10A* locus, further cementing the central role for this genomic region in BrS genetic pathogenesis.[5] All lead variants are noncoding and located in or near regulatory elements (REs) at the *SCN5A–SCN10A* locus that have been characterized in detail (Figure 1A), including the *SCN5A* promoter, a downstream superenhancer encompassing RE6 through RE9 and 2 intragenic *SCN5A* enhancer elements (RE4/RE5).[6,7] A short transcript of *SCN10A*, comprising the last 7 exons and controlled by an intronic enhancer (RE1–RE2)–promoter complex, is expressed in the heart.[8] A common variant in RE1 associated with BrS and ECG traits, rs6801957, leads to reduced expression of *SCN10A*-short and decreased cardiac I_{Na} while minimally affecting *SCN5A* expression.[8]

BrS is several times more prevalent in East (especially Southeast) Asia compared with regions of predominantly European ancestry. After its initial description in 1992,[9] BrS was recognized as the major cause of sudden unexplained death syndrome in Thailand, a condition causing sudden nocturnal death in young men and traditionally known locally as *Lai Tai*.[10,11] The high rate of BrS in Southeast Asia is not attributable to an increased prevalence of ultrarare loss-of-function *SCN5A* coding variants; indeed, a relatively lower diagnostic yield is observed compared with European ancestry cases (≈5% versus 20%).[2,12] We previously demonstrated enrichment of a low-frequency *SCN5A* coding variant of intermediate effect size, p.Arg965Cys, in Thai patients with BrS compared with population-matched controls.[12] However, other genetic factors underlying the higher prevalence of BrS in Southeast Asia are still largely unknown. Here, we identify and functionally validate a novel rare noncoding variant in an *SCN5A* enhancer that is highly enriched in patients with BrS from Thailand and partly explains the increased prevalence of BrS in this region.

METHODS

Data Availability

The RNA sequencing data set is available in the Gene Expression Omnibus database (accession record GSE264359).

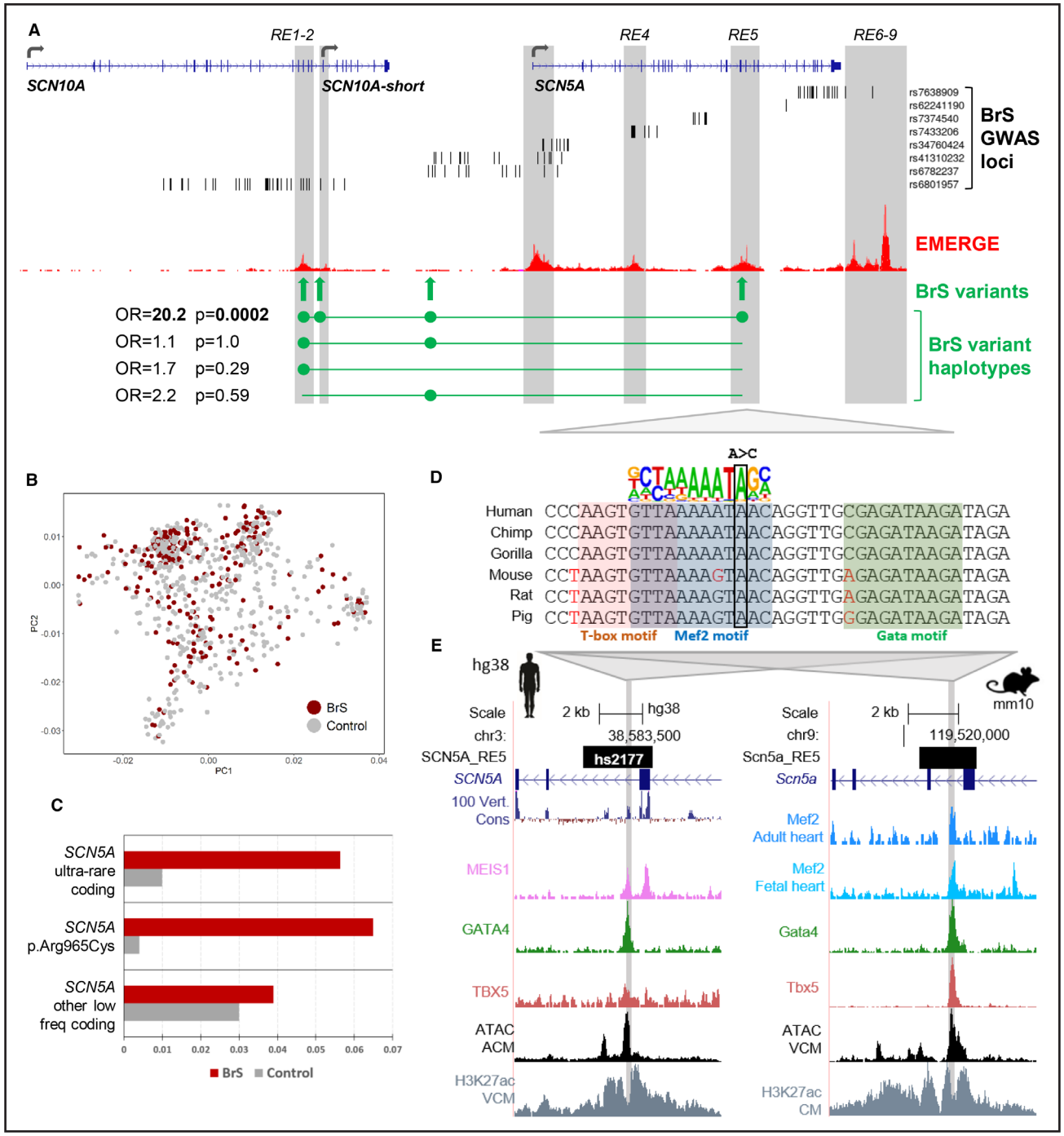

Figure 1. Identification of a noncoding enhancer variant in SCN5A associated with BrS.
A, Overview of the coding sequence and regulatory elements at the *SCN10A–SCN5A* locus, highlighting single nucleotide polymorphisms (SNPs) from Brugada syndrome (BrS) genome-wide association study (GWAS; lead SNP and SNPs with r^2>0.5 in European populations), the EMERGE track of cardiac-specific epigenetic markers, the location of the 4 rare and low-frequency noncoding variants associated with BrS in Thai patients, and odds ratios (ORs) and *P* values for each haplotype. **B**, Principal component analysis for patients with BrS and controls from Thailand. **C**, BrS case and control frequencies for *SCN5A* coding variants: ultrarare variants (gnomAD filtering allele frequency <0.00001), the low-frequency variant p.Arg965Cys, and other low-frequency variants (gnomAD filtering allele frequency <0.001). **D**, Sequence alignment of 6 mammalian species, including human and mouse, of the hs2177 enhancer core that encompasses the GRCh38:3-38580380-A-C variant (indicated by box). The variant is located in and disrupts a predicted and conserved Mef2 motif site (indicated by blue shading) and is flanked by T-box (red shading) and Gata (green shading) recognition sites as predicted by Homer. **E**, UCSC browser views of the hs2177-*SCN5A* RE5 enhancer in human (hg38) and mouse (mm10). Relevant cardiac transcription factor chromatin immunoprecipitation sequencing and assay for transposase-accessible chromatin with sequencing traces from the literature were plotted (see Table S1 for data set references). ACM indicates atrial cardiomyocytes; CM, cardiomyocytes; and VCM, ventricular cardiomyocytes.

All other supporting data are available within the article and in the Supplemental Material.

BrS and Control Cohorts

The patients with BrS were recruited from 7 participating institutions in Thailand. All patients were diagnosed with BrS according to the 2013 Heart Rhythm Society/European Heart Rhythm Association/Asia Pacific Heart Rhythm Society Expert consensus statement.[13] Blood samples were collected for DNA extraction and genotyping. The control samples were collected from volunteers who had no Brugada pattern (type 1) on standard 12-lead ECG. All patients and controls were of Thai ethnic origin by self-report. The study was approved by the institutional review board of the faculty of medicine, Chulalongkorn University, Bangkok, Thailand (institutional review board no. 431/58). Informed consent was obtained from all participants. All methods were performed in accordance with relevant guidelines or regulations.

Genome Sequencing and Analysis

Data Generation and Processing

The samples were sequenced by the Illumina FastTrack service on HiSeqX with a PCR-free library. Data processing, alignment, and variant calling were performed using standardized approaches as described in the Methods in the Supplemental Material. Samples were excluded on the basis of a missing genotype rate of >0.03, relatedness (PI_HAT>0.2; 1 of related sample group retained with priority for cases), high inbreeding rate (F>0.1), or sex check inconsistencies. Sample ancestry was determined using principal component analysis (PCA) with samples from the 1000 Genomes (1KG) data set. All samples clustered with East Asian 1KG samples. A PCA of cases and controls was plotted to demonstrate ancestry matching.

Genetic Variant Analysis

All *SCN5A* coding variants were described with respect to the ENST00000333535 transcript. Coding variants were classified using the guidelines of the American College of Medical Genetics and Genomics and the Association for Molecular Pathology[14] as previously described.[2] Noncoding variants at the *SCN5A–SCN10A* locus were assessed for enrichment in cases versus controls using Fisher exact test (for samples with or without variants). The following regulatory regions at the locus were queried for variants (all coordinates based on GRCh38): RE1/*SCN10A* enhancer (chr3:38725264-38728203), RE2/*SCN10A* enhancer (chr3:38721868-38725264), *SCN10A*-short promoter (chr3:38716810-38719605), *SCN5A* promoter (chr3:38642253-38652554), RE4/*SCN5A* enhancer (chr3:38613169-38618856), RE5/*SCN5A* enhancer (chr3:38575835-38584663), and RE6-9/*SCN5A* superenhancer (chr3:38526650-38546621), as well as the intermediate sequence between these regions (Figure 1A).[6] To assess for linkage disequilibrium between variants, r^2 values were calculated for each variant pair in this region (with a combined minimum case and control allele count of 3). Variants of interest were further annotated with CADD and FINSURF scores,[15] frequency in gnomADv3 East Asian genome sequences (n=2604), and conservation of affected base across species using Ensembl version 109. The frequency of the putative causal variant was also assessed in other genomic databases with individuals of Asian ancestry: the Genomics Thailand database of 10 043 individuals of Thai ancestry; the Singaporean SG10K_Health v5.3 database of individuals of Chinese, Indian, or Malay ancestry[16]; the jMORP/54KJPN database of individuals of Japanese ancestry[17]; and the KOVA database of individuals of Korean ancestry.[18]

Transcription Factor Motif Analysis

Transcription factor (TF) motif scanning analysis was performed using Homer[19] to detect the presence of 1847 motifs in the Homer[19] and Jaspar[20] databases for the wild-type and variant sequences in the enhancer region of interest. The enhancer region was further characterized using human and mouse chromatin immunoprecipitation sequencing data sets (Table S1).

Generation of Human Induced Pluripotent Stem Cell–Derived Cardiomyocytes

hiPSC Culture, Genome Editing, and Characterization of Clones

The Personal Genome Project 1 human induced pluripotent stem cell (hiPSC) line, PGP1-SV1, referred to as PGP1 in this article (detailed information is available at https://arep.med.harvard.edu/gmc/PGP_cells.html), as well as the derived edited clones, were maintained on growth factor–reduced Matrigel Matrix (Corning)–coated plates in presence of mTeSR1 medium (Stemcell Technologies). Cells were passaged every 3 to 4 days using 0.5 mM EDTA (Life Technologies) in PBS without $CaCl_2$ and $MgCl_2$ and replated in presence of Rho kinase inhibitor (Fasudil HCl; Selleck Chemicals) for the first 24 hours. Cells were maintained at 37 °C, with 5% CO_2 and 20% O_2. The RE5 GRCh38:chr3-38580380-A-C variant was introduced in heterozygous state in the PGP1 hiPSC line by CRISPR/Cas9-mediated editing (Synthego). The Cas9 and gRNA, as ribonucleoprotein, and the single strand oligodeoxynucleotide carrying the single nucleotide variant for homology-directed repair (sequences in Table S2) were introduced by nucleofection. Two heterozygous, edited clones (A7 and C8) were selected after Sanger sequencing of their genomic DNA (primers in Table S2 and Figure S2A). Quality controls were performed on these edited clones, which confirmed karyotype integrity by KaryoStat Assay (Figure S2B) and pluripotency by PluriTest Assay (Figure S2C; Synthego). One predicted off-target genomic locus, exhibiting 2 mismatches with the guideRNA spacer sequence, was identified by the Wellcome Sanger Institute Genome Editing off-target finding tool (https://wge.stemcell.sanger.ac.uk/find_off_targets_by_seq) at position GRCh38:chr8-15043569-15043591. An ≈200-bp window of genomic DNA from the A7 and C8 clones, centered around this predicted potential off-target site, was sequenced by Sanger sequencing to detect any sequence alterations (primer sequences in Table S2). No sequence alterations were detected in in the 2 edited clones (A7 and C8).

hiPSC–Derived Cardiomyocytes Generation

The parental PGP1 and edited A7 and C8 hiPSC lines were maintained in undifferentiated state in presence of mTeRS1 medium on Matrigel Matrix-coated plates until they reached 65% to 80% confluence. Differentiation into cardiomyocytes was then performed as described by Maas et al[21] without cardiomyocytes expansion and with modifications described in the Methods in the Supplemental Material. The efficacy of the

cardiomyocyte differentiation, and the consistency between the wild-type and edited lines, was demonstrated through RNA sequencing data for cardiomyocyte differentiation and maturation-relevant genes, as well as the expression ratio of the "fetal" and "adult" *SCN5A* exon 6 (Figure S3).

RNA Sequencing

RNA Isolation

Total RNA was isolated from hiPSC–derived cardiomyocytes (hiPSC-CMs) derived from 4 independent batches of differentiation of the parental PGP1 and heterozygous RE5 variant–carrying A7 hiPSC isogenic lines. Cardiomyocyte cultures were lysed by TRIzol Reagent (Ambion/Life Technologies) followed by chloroform addition (200 µL/mL of TRIzol Reagent) and hydrophilic phase isolation after centrifugation at 4 °C. RNA was then precipitated in presence of isopropanol, pelleted by centrifugation at 4 °C, and washed twice with 75% ethanol. The RNA pellet was then briefly air-dried and resuspended in RNase-free water.

Determination of Phase Between the RE5 Variant and an Exonic SNP

To determine the *SCN5A* transcript output from each allele of the A7 and PGP1 lines using bulk messenger RNA sequencing analysis, we took advantage of the presence of a heterozygous SNP (GRCh38:3-38580976-T-C; rs7430407) in *SCN5A* exon 17. The phase between the SNP and the RE5 variant in the A7 line was determined by amplifying an 802 base pair region encompassing the 596-bp interval between the rs7430407 SNP and the RE5 variant (primers in Table S2), followed by cloning and Sanger sequencing. This demonstrated that the C-allele of the RE5 variant was in cis with the C-allele of rs7430407 (Figure 2B).

Bulk RNA Sequencing and Analysis

Quality and integrity of the isolated RNA was determined by 4200 TapeStation (Agilent) analysis, which indicated a RIN score >9 for all samples. Cardiomyocytes from the parental PGP1 and isogenic A7 hiPSC lines were used for bulk RNA sequencing. Library preparations were made after ribosomal RNA depletion by KAPA Total RNA HyperPrep with RiboErase kit (Roche). Sequencing was performed on an Illumina platform NovaSeq S4.300 in pair-end mode with read length of 150 bp (PE150) and a sequencing depth of 60 million reads per sample. We used STAR[22] to map reads to the hg19 build of the human genome/transcriptome. We used VarScan 2[23] to detect variants and their allele-specific occurrence within the samples. We used a minimum base quality Phred score of 15, a minimum read depth of 10, and a minimum variant allele frequency threshold of 0.20 in VarScan 2 for variant detection. To determine whether a variant was specifically enriched or depleted in either cell line, indicative for allele-specific enhancer activity, a *Z* test was performed on the observed allele frequencies ($P<0.05$; *Z* test).[24]

Electrophysiology Patch Clamp Analysis

Single-Cell Electrophysiology Data Acquisition

The hiPSC-CM cultures were dissociated to obtain single cardiomyocytes as described in the Methods in the Supplemental Material. I_{Na} was recorded from hiPSC-CMs using an Axopatch 200B amplifier (Molecular Devices). Voltage control, data acquisition, and analysis were realized with custom software.[25] Signals were low-pass–filtered with a cutoff of 5 kHz and digitized at 20 kHz. Cell membrane capacitance (C_m) was calculated by dividing the time constant of the decay of the capacitive transient after a −5 mV voltage step from −40 mV by the series resistance. Series resistance was compensated for by at least 80%. Following the procedure of Veerman et al,[26] we selected single, spontaneously beating hiPSC-CMs showing regular, synchronous contractions in modified Tyrode solution, after which this extracellular solution was switched to a solution suitable for specific I_{Na} measurements. Modified Tyrode solution contained the following (in mmol/L): NaCl 140, KCl 5.4, $CaCl_2$ 1.8, $MgCl_2$ 1.0, glucose 5.5, HEPES 5.0, with pH 7.4 (NaOH).

Sodium Current Measurements

I_{Na} was recorded at room temperature (≈20 °C) using the ruptured patch-clamp technique. Extracellular solution contained the following (in mmol/L): NaCl 20, CsCl 120, $CaCl_2$ 1.8, $MgCl_2$ 1.0, glucose 5.5, HEPES 5.0, with pH 7.4 (CsOH). Nifedipine (10 µmol/L; Sigma) was added to block the L-type Ca^{2+} current in hiPSC-CMs.[27] Patch pipettes were pulled from borosilicate glass (GC100F-10; Harvard Apparatus) and had resistances of ≈2.5 MΩ after filling with the solution consisting of (in mmol/L) NaCl 3.0, CsCl 133, $MgCl_2$ 2.0, Na_2ATP 2.0, TEACl 2.0, EGTA 10, and HEPES 5.0, with pH 7.2 (CsOH). I_{Na} was measured using a double pulse protocol from a holding potential of −120 mV (Figure 2D, inset; cycle length of 5 seconds). The first pulse was used to determine the I–V relationship and voltage dependency of activation; the second pulse was used to analyze the voltage dependency of inactivation. I_{Na} was defined as the difference between peak and steady-state current and current densities were calculated by dividing current amplitude by C_m. Voltage dependence of activation and inactivation curves were fitted with Boltzmann function ($I/I_{max}=A/\{1.0+\exp[(V_{1/2}-V)/k]\}$), where $V_{1/2}$ is the half-maximal voltage of (in)activation and k the slope factor (in mV). The time course of current inactivation was fitted by a double-exponential equation: $I/I_{max}=A_f\times\exp(-t/\tau_f)+A_s\times\exp(-t/\tau_s)$, where A_f and A_s are the fractions of the fast and slow inactivation components, and τ_f and τ_s are the time constants of the fast and slow inactivating components, respectively.

Statistical Analysis

Clinical Characteristics Statistical Analysis

Clinical characteristics including demographic data, history of cardiac events, and ECG measures were compared among the 4 genotype groups (RE5 variant, ultrarare *SCN5A* coding variants, *SCN5A*:p.Arg965Cys, and no low-frequency *SCN5A* coding variants). Statistical analyses were performed using χ^2 or Fisher exact tests for categorical variables and ANOVA for continuous variables.

Electrophysiology Patch Clamp Statistical Analysis

Data are expressed as mean±SEM, unless stated otherwise. Statistical analysis was carried out with SigmaStat 3.5 software (Systat Software, Inc.). Normality and equal variance assumptions were tested with the Kolmogorov-Smirnov and the Levene median test, respectively. Significance between measures was tested using 1-way repeated-measures ANOVA followed by pairwise comparison using the Student-Newman-Keuls test

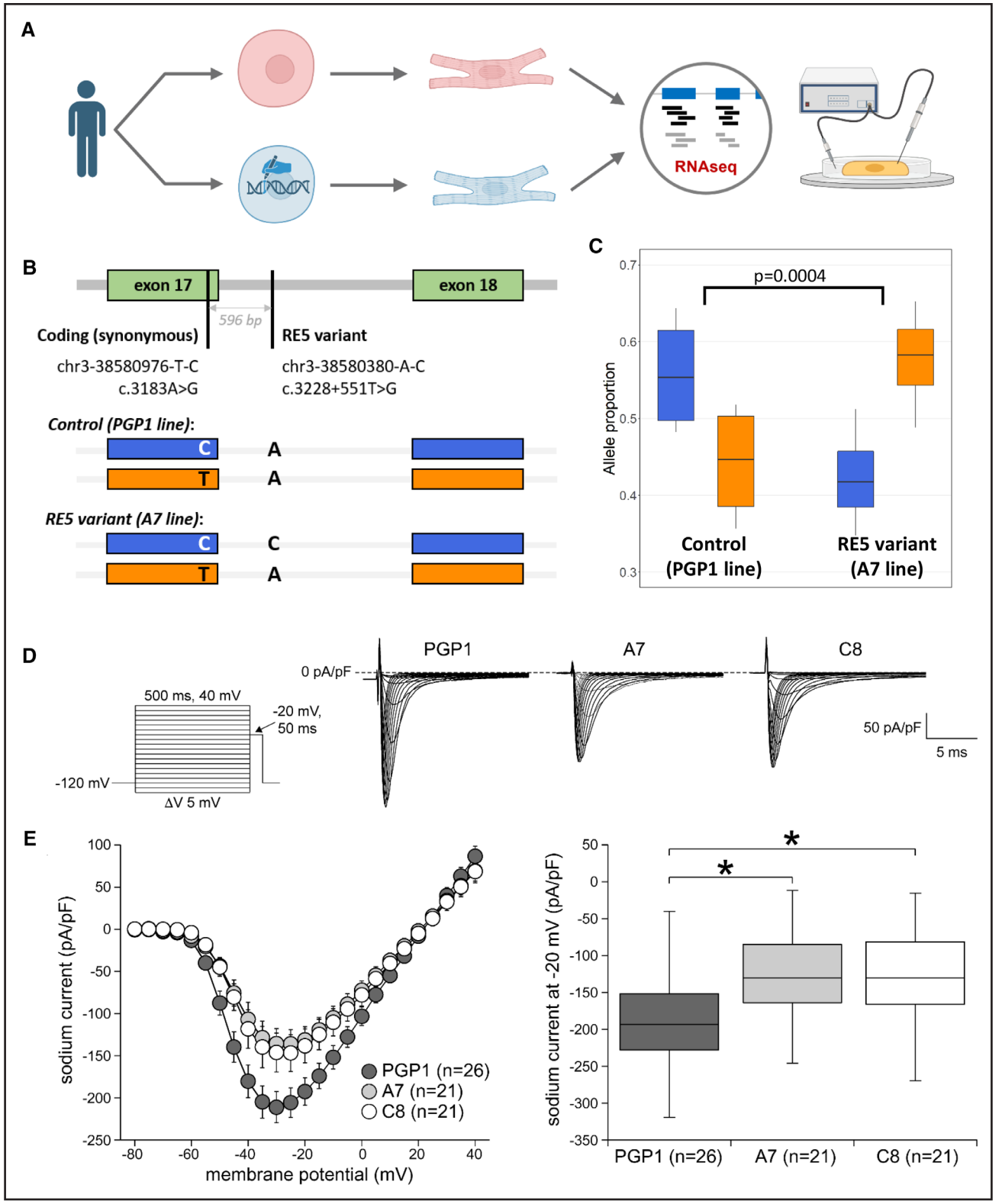

Figure 2. Experimental characterization of the RE5 variant.

A, Overview of experimental validation: generation of human induced pluripotent stem cell–derived cardiomyocytes (hiPSC-CMs) from PGP1 cell line, isogenic control (red), and RE5 variant line (blue), where the variant was introduced in the heterozygous state by CRISPR-Cas9 editing (graphic produced with BioRender). **B**, Allelic balance of *SCN5A* expression in the 2 lines was assessed using the heterozygous synonymous coding variant c.3183A>G present in the PGP1 line (596 bases upstream of the RE5 variant in exon 17), with the C exonic allele demonstrated to be in phase with the RE5 variant. **C**, Allelic balance of SCN5A expression in the control and RE5 variant lines as determined by RNA sequencing (4 biological replicates each), where *P* value refers to the *Z* test differences in allelic expression ratios. **D**, Sodium current (I_{Na}) characterization in control hiPSC-CMs (PGP1; 26 cells from 6 differentiations) and hiPSC-CMs of the 2 RE5 variant lines (A7, 21 cells from 6 differentiations; and (*Continued*)

Figure 2 Continued. C8, 21 cells from 5 differentiations), showing representative traces of I_{Na} activated during the first depolarizing pulses of the voltage clamp protocol shown in the inset. **E**, Average current–voltage (I-V) relationships of peak I_{Na} (**left**) and boxplots depicting I_{Na} densities (median and boxes represent interquartile range), determined at −20 mV (**right**). *Significance compared with controls ($P<0.05$; Kruskal-Wallis test, followed by Dunn comparisons).

or by the Kruskal-Wallis test followed by pairwise comparisons with Dunn method. $P<0.05$ defines statistical significance.

RESULTS

Identification of Rare Noncoding Variants at *SCN5A–SCN10A* Locus

Genome sequencing data were generated for BrS probands and controls from Thailand (see Methods for details of data generation, read mapping, variant calling, and quality control checks). After sample-level quality control, a total of 231 unrelated probands and 500 ancestry-matched controls were included, with principal component analysis demonstrating the cohorts were of comparable ancestral background (Figure 1B). Of 231 BrS probands (mean age, 47.6±12.8 years; 95% male), 88% had a documented spontaneous BrS ECG pattern and 76% were symptomatic (Table 1). A total of 5.6% of cases had an ultrarare (gnomAD filtering allele frequency <0.00001) *SCN5A* coding variant (versus 1.0% in controls; $P=4.0E-04$), 6.5% carried the *SCN5A*:p.Arg965Cys low-frequency variant (versus 0.4% in controls; $P=1.6E-06$), and 3.9% had other low-frequency (gnomAD filtering allele frequency <0.001) *SCN5A* coding variants, although the latter were only marginally enriched over controls (3.0%; $P=0.51$; Figure 1C; Table S3).

Rare and low-frequency noncoding variants at the *SCN5A-SCN10A* locus encompassing the defined promoter and enhancer regions were assessed for enrichment in BrS probands versus controls. Four variants in linkage disequilibrium ($r^2>0.2$) were identified (Table 2): chr3-38580380-A-C in the *SCN5A* enhancer RE5, chr3-38719550-C-T in the *SCN10A*-short transcript promoter, chr3-38724980-T-C in the *SCN10A*-short enhancer RE2, and chr3-38683338-C-T in the intergenic region between *SCN5A* and *SCN10A* (Figure 1A; GRCh38 coordinates).

For these 4 variants, the largest case-control odds ratios (ORs) were observed for the RE5 and *SCN10A*-short promoter variants (in complete linkage disequilibrium in this data set). Haplotypes containing only one or both of the RE2 and intergenic variants had no association with BrS, confirming they are merely tagging the causal variant (Figure 1A). The RE5 variant alters a nucleotide fully conserved across 35 mammalian species with available orthologous sequence data, in contrast to the other 3 variants (Figure S1), and has higher computational deleteriousness scores from the CADD and FINSURF[15] algorithms (Table 2). The RE5 variant is also

Table 1. Clinical Characteristics of Participants Grouped According to *SCN5A* Genotype

Characteristics	All cases (n=231)	RE5 variant (n=9)	Ultrarare coding variant (n=13)	p.Arg965Cys (n=15)	*SCN5A* variant negative (n=186)
Male sex	220 (95)	9 (100)	13 (100)	15 (100)	175 (94)
Age, y	47.6±12.8	48.9±12.9	45.1±13.7	49.7±12.7	47.7±12.7
Spontaneous BrS ECG pattern	166 (89)	8 (89)	8 (89)	13 (100)	130 (87)
Symptomatic	173 (75)	8 (89)	10 (77)	10 (67)	141 (76)
SCA/VT/VF	134 (58)	8 (89)	7 (54)	10 (67)	108 (58)
Syncope	78 (34)	4 (44)	6 (46)	4 (27)	63 (34)
FH of SCA/SCD	81 (42)	3 (33)	6 (60)	5 (33)	66 (43)
ECG measures					
Cases with ECG data, n	187	8	9	13	150
RR interval, ms	853±171	846±117	892±169	869±161	846±176
PR interval, ms	177±29	181±28	187±33	191±32	175±29
QRS duration, ms	109±19	111±25	110±18	111±12	109±20
QT interval, ms	432±44	434±39	409±27	438±33	433±46
QRS axis, °	44±51	7.88±52	55.4±29	37.4±47	46.4±51
Left QRS axis deviation	16 (9)	2 (25)	0 (0)	1 (8)	12 (8)

Values are n (%) or mean±SD. Nine patients with low-frequency *SCN5A* coding variants other than p.Arg965Cys were not evaluated separately (Table S3). One patient carried both the p.Arg965Cys variant and the ultrarare coding variant p.Gly638Asp. Clinical data are available for all 231 Brugada syndrome (BrS) cases, except for spontaneous BrS ECG pattern (n=187 cases only), family history (FH) of sudden cardiac arrest (SCA)/sudden cardiac death (SCD; n=193 cases only), and ECG measures (case numbers as shown). For incomplete clinical data, the percentages reflect cases in which data are available. VF indicates ventricular fibrillation; and VT, ventricular tachycardia.

Table 2. Details of the Noncoding Variants at the SCN5A-SCN10A Locus Associated With BrS in Patients and Controls From Thailand

Variant (GRCh38)	Location	Case frequency, %	Control frequency, %	*P* value	OR (95% CI)	gnomADv3 EAS MAF	FINSURF score	CADD score	r^2 (RE5)
3-38580380-A-C	RE5 enhancer	3.9	0.2	2.0E-04	20.2 (2.5–160.6)	–	0.82	14.7	–
3-38719550-C-T	SCN10A–short promoter	3.9	0.2	2.0E-04	20.2 (2.5–160.6)	0.00116	–	2.2	1.0
3-38724980-T-C	RE2 enhancer	7.4	2.4	3.4E-03	3.2 (1.5–6.9)	0.00077	0.08	2.4	0.34
3-38683338-C-T	Intergenic	5.2	1.0	9.7E-04	5.4 (1.9–15.6)	–	–	0.5	0.59

Details including location with respect to *SCN5A*/*SCN10A* regulatory elements, sample-level frequencies in cases (n=231) and controls (n=500), Fisher exact test *P* values, odds ratios (ORs) with 95% CI, minor allele frequencies (MAF) in gnomADv3 East Asian (EAS) individuals, FINSURF score (a machine-learning approach to predict the functional effect of noncoding variants in regulatory regions; score ranges from 0 to 1 with increasing deleteriousness),[15] CADD scores, and r^2 values of linkage disequilibrium with respect to the RE5 variant (calculated from the patient and control data in this study).

absent in the gnomADv3 database (n=76 165 genomes, including n=2604 of East Asian ancestry), whereas the *SCN10A*-short promoter variant has a gnomAD–East Asian frequency of 0.001, indicating it also exists on haplotypes distinct from the RE5 variant. Based on this cumulative evidence, the RE5 variant was deemed to be the putative causal variant for this risk haplotype.

The RE5 variant was detected in 3.9% (n=9) of cases versus 0.2% (n=1) of controls (*P*=2.0E-04; OR, 20.2 [2.5–160.6]). We searched the Genomics Thailand database, comprising 10 043 individuals with a range of clinical and pharmacogenetics indications (https://genomicsthailand.com/Genomic/home), to attain a more precise estimate of the variant frequency in Thailand. It was detected in 6 individuals (0.06%), yielding an OR of 45.2 (14.5–141.3) compared with the BrS cohort (*P*=5.6E-12). In addition to gnomADv3–East Asian, the RE5 variant is also not detected in other genomic data sets of Asian ancestry (comprising 87 867 individuals; Table S4), suggesting it is restricted to Thai or Southeast Asian populations.

Clinical Characterization of RE5 Variant Carriers

None of the 9 patients with BrS with the RE5 variant had rare or low-frequency coding variants in *SCN5A*. When grouping cases by genotype (ie, RE5 variant, ultrarare *SCN5A* coding variants, *SCN5A*:p.Arg965Cys, no low-frequency [gnomAD filtering allele frequency <0.001] *SCN5A* coding variants), no statistically significant differences in clinical characteristics were observed (Table 1), although a significant leftward shift of ECG QRS axis was observed in cases with the RE5 variant (7.88±52° versus 46.4±51°; *P*<0.05), with 2 cases displaying left QRS axis deviation (−30° to −150°).

Patients with the RE5 variant were particularly symptomatic: 89% (8/9) had a history of sudden cardiac arrest, 7 of whom had documented ventricular tachycardia or ventricular fibrillation, compared with only 58% of cases without any *SCN5A* variant (Table S5). For one patient, analysis of their family pedigree revealed the variant largely segregated with phenotype, although one genotype-negative individual displayed a drug-induced BrS ECG pattern (Figure 3A). However, this should be interpreted in the context of an appreciable false-positive rate for this test,[28] and the fact that it is not atypical in BrS families for individuals lacking the familial pathogenic *SCN5A* variant to be phenotype-positive due to the complex genetic pathogenesis of the disease.[29]

Three patients with the RE5 variant underwent epicardial substrate ablation using the sodium channel blocker ajmaline to define the substrate areas of the right ventricular outflow tract and right ventricular inferior epicardium.[30] These procedures revealed large substrate areas more similar to *SCN5A*-positive than *SCN5A*-negative cases,[31] suggesting a substantial loss-of-function effect of the RE5 variant (Figure 3B and 3C).

Functional Validation of the RE5 Variant

To assess the potential consequences of the RE5 variant, we performed a transcription factor (TF) motif scanning analysis using Homer[19] on a 1286 base pair stretch of the hs2177 enhancer sequence[32] (which is fully encompassed by the RE5 region and includes the variant site), scanning for the presence of 1847 motifs in the Homer[19] and Jaspar[20] databases. Nine variant-dependent motif recognition sites were detected: 8 exclusive to the wild-type sequence and 1 to the RE5 variant sequence (Table S6). Of the 8 sites lost by the RE5 variant, 6 are different representations of the Mef2 motif (CTAWWWWTAG; −5 to +5). The variant substitutes the A nucleotide at position +4 of the motif, previously shown to cause a strong reduction in binding affinity for Mef2.[33] This Mef2 binding sequence is conserved in evolution and its functionality is supported by Mef2 chromatin immunoprecipitation sequencing data from mouse hearts[34] (Figure 1D and 1E; Figure S4A). The motif gained by the RE5 variant represents a binding site for the Gfi1B transcriptional repressor.[35]

The effect of the RE5 variant on expression, and specifically through loss of Mef2 binding, was assessed using luciferase assays in hiPSC-CMs (which endogenously express cardiac-specific TFs including Mef2) and HEK-293 cells (using cotransfection with Mef2C and Myocardin, a Mef2 coactivator; see the Methods in the Supplemental Material). The wild-type RE5

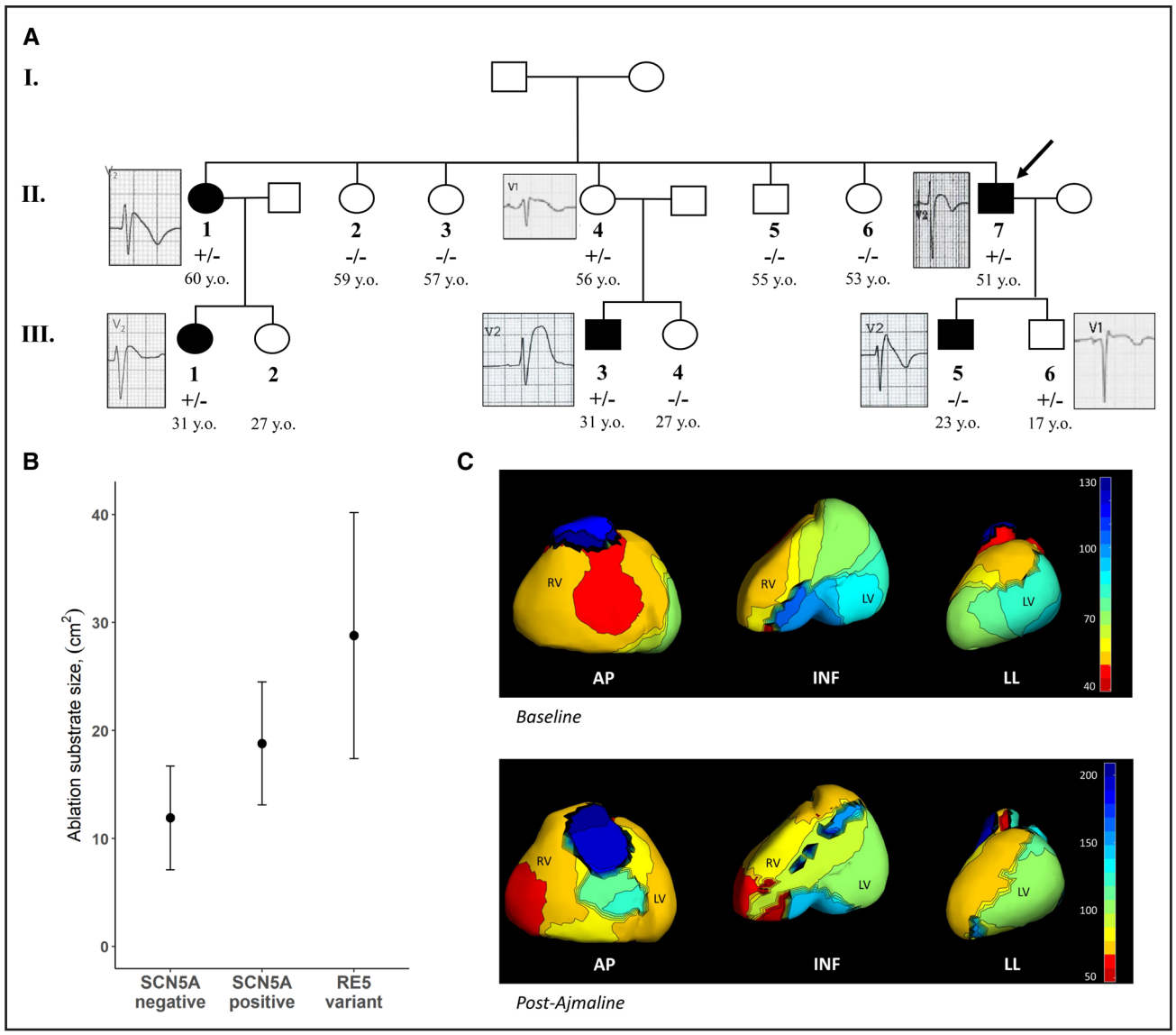

Figure 3. Clinical aspects of carriers of the RE5 variant.

A, Family pedigree of one of the patients with Brugada syndrome (BrS) carrying the RE5 variant with ages indicated (the proband is II-7, as indicated). Three family members with the variant tested positive for BrS after ajmaline challenge (II-1, III-1, III-3; black fill). Two other family members with the variant did not consent to ajmaline challenge: II-4 displayed a borderline baseline Brugada type I pattern and III-6 displayed a baseline Brugada type III pattern. One individual also tested positive for BrS after ajmaline challenge despite not carrying the RE5 variant (III-5), which is not atypical for *SCN5A* pathogenic variants in BrS families and reflects the complex genetic pathogenesis of the disease. No other noncarriers display the Brugada marker on ECG. **B**, Epicardial substrate ablation areas (after ajmaline challenge) for patients with BrS carrying the RE5 variant (n=3; substrate sizes 40.0, 29.2, and 17.2 cm^2; mean±SD, 28.7±11.5 cm^2) compared with data from Ciconte et al[31] for carriers of pathogenic coding variants in *SCN5A* (*SCN5A*-positive; n=49; mean±SD, 18.8±5.7 cm^2) and patients with BrS without *SCN5A* variants (*SCN5A*-negative; n=146; mean±SD, 11.9±4.8 cm^2; 1-way ANOVA, $P<0.0001$; Tukey honestly significant difference post hoc for RE5 vs *SCN5A*-negative, $P<0.0001$).[31] **C**, Baseline (above) and postajmaline (below) epicardial mapping for the proband of the pedigree in **A**, with the color bar representing local activation time from early (red) to late (blue) activation (scale in milliseconds). The latest activation was localized at the right ventricular outflow tract (RVOT), the target for radiofrequency ablation, before and after ajmaline administration. However, the latest activation at the RVOT was markedly prolonged after ajmaline, increasing from 130 ms before to 200 ms after. AP indicates anterior-posterior; INF, inferior; LL, left lateral; LV, left ventricle; and RV, right ventricle.

fragment drove robust luciferase activity in both the hiPSC-CMs and HEK-293 cells, whereas the RE5 variant allele showed significantly lower reporter gene activity (Figure S4B and S4C).

To evaluate the functional consequences of the presence of the RE5 variant in the context of a human cardiomyocyte, we introduced the heterozygous variant into a hiPSC line. The PGP1 hiPSC line (details in Methods) was edited by the CRISPR/Cas9-mediated homology-directed repair method and 2 isogenic clones (A7 and C8) carrying the single nucleotide variant in heterozygous form were isolated and characterized (Figure S2). hiPSC-CMs from the parental and heterozygous mutant lines were generated by adaptation of a protocol based

on small molecules–mediated modulation of the cWnt pathway[21] (details in Methods).

We evaluated the potential cis-regulatory effect of the RE5 variant on *SCN5A* allelic expression through RNA sequencing analysis of hiPSC-CMs from the A7 variant line and the isogenic control (PGP1). To distinguish transcripts originating from the 2 alleles, we took advantage of the presence of a heterozygous SNP located in an exon adjacent to the RE5 intronic variant (rs7430407, GRCh38:3-38580976-T-C, located 596 bases from the RE5 variant) and determined their phase in the A7 line (details in Methods; Figure 2B). The allele-specific transcript output ratios in the hiPSC-CMs of the 2 isogenic lines (PGP1 and A7) were quantified and compared, with A7 hiPSC-CMs containing the RE5 variant displaying a 34% reduction of the *SCN5A* transcript allelic ratio compared with PGP1 controls (*Z* test, *P*=0.0004; Figure 2C; Table S7). This method of comparing the allelic balance between the wild-type and variant alleles, within each cell line and RNA sequencing sample, controls for the expected variability between samples to more accurately gauge the effect of the variant on *SCN5A* expression. However, the overall normalized *SCN5A* expression also shows a 28% reduction in the RE5 variant line. In mice, the 2 *Scn5a* alleles are independently regulated.[6] These data further indicate allele-specific reduced RE5 enhancer activity and *SCN5A* expression due to loss of the Mef2 motif as a consequence of the variant.

I_{Na} measurements were performed in control hiPSC-CMs (PGP1) and in the hiPSC-CMs of the 2 isogenic lines (A7 and C8) with the RE5 variant. Figure 2D shows typical I_{Na} recordings (−80 to 0 mV) from all groups and Figure 2E (left) shows the average current–voltage (I–V) relationships of I_{Na}. The I_{Na} density was significantly lower in hiPSC-CMs of both RE5 variant lines, with a 30% reduction at −20 mV (Figure 2E, right). Neither the voltage dependency of activation (Figure S5A) nor the voltage dependency of inactivation (Figure S5B) were affected by the RE5 variant. The time constants of current inactivation, determined at a test potential of −20 mV, were not different in hiPSC-CMs of the 2 RE5 variant lines compared with the control (data not shown). Action potential measures were not assessed, but because the action potential upstroke velocity in cardiomyocytes (see Berecki et al[36] and primary references cited therein), including hiPSC-CMs (Figure S6), is strongly regulated by I_{Na} density (or availability), a 30% reduction in I_{Na} density would result in a 24% reduced upstroke velocity. In summary, the RE5 variant results in a decrease in I_{Na} density without changes in gating properties, concordant with the reduced *SCN5A* expression from the allele harboring the RE5 variant.

DISCUSSION

In this study, we have identified and validated a rare noncoding *SCN5A* enhancer variant associated with BrS in Thailand, one of the first examples of a rare regulatory variant of proven pathogenicity in a cardiac disease gene. The variant is highly enriched in patients with BrS, with an OR between 20 and 45 based on our study controls and the Genomics Thailand database, respectively, and is located within a characterized enhancer region for *SCN5A* (RE5). Computational evidence was highly supportive of pathogenicity, based on deleteriousness scores of the CADD and FINSURF algorithms, full conservation of the affected nucleotide base, and the predicted disruption of a Mef2 TF binding site. The causality of the variant was subsequently confirmed by the demonstration of a significant reduction in both allele-specific *SCN5A* expression and $Na_v1.5$ sodium channel function in CRISPR-Cas9–edited hiPSC-CMs compared with isogenic controls. These effects are consistent with the loss-of-function mechanism of action of known pathogenic BrS coding variants in *SCN5A* (either missense or protein-truncating variants). The frequency of the variant in cases, its apparent specificity to the Thai population, alongside its demonstrated functional effect, suggest that it is an important contributor to the high prevalence of the disorder in Thailand.

The diagnostic yield for clinical genetic testing in patients with BrS from Thailand (ie, ultrarare loss-of-function coding variants in *SCN5A*) is several fold lower than in patients with BrS of European ancestry (5% versus 20%). This likely reflects the increased prevalence of BrS in this region (ie, whereas the relative rate is lower, the absolute rate of such variants is expected to be broadly similar across populations in the absence of specific founder variants; Figure 4). We previously described a 9% yield in Japanese patients with BrS, which reflects a disease prevalence intermediate between Europe and Southeast Asia.[2] Because the RE5 variant is found in ≈1 in every 25 patients with BrS from Thailand, it may partly explain the increased prevalence of this condition in this region, in conjunction with the *SCN5A*:p.Arg965Cys intermediate effect variant we previously described (present in 6.5% of cases; Figure 4). Indeed, the RE5 variant accounts for almost as many Thai patients with BrS as all of the ultrarare *SCN5A* coding variants combined and a relatively equivalent proportion of patients with BrS of European ancestry with causal *SCN5A* coding variants.

The strong observed effect size of this variant (based on both case–control OR and functional analysis) is reflected in the severe phenotype observed in BrS carriers and may be explained by the predicted concurrent loss of a Mef2 motif (a critical family of cardiac TFs) and possible gain of a Gfi1 transcriptional repressor, although further studies will be needed to probe the exact transcriptional mechanisms underlying *SCN5A* downregulation. The 30% reduction in I_{Na} caused by the RE5 variant is a remarkably strong effect for a single nucleotide variant in a noncoding regulatory region, given the complex regulatory machinery at the *SCN5A* gene, which encompasses numerous promoter and enhancer regions. By comparison,

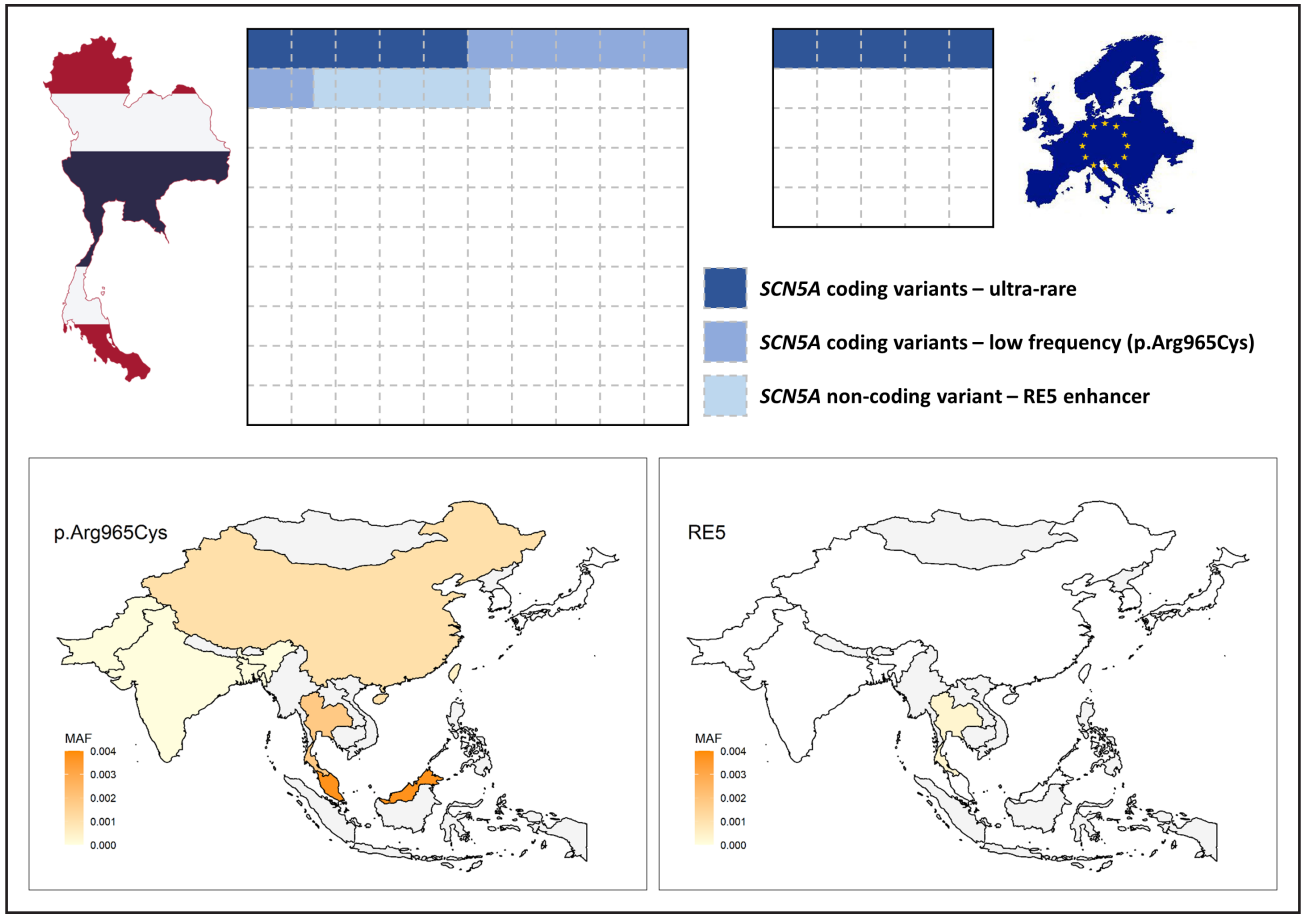

Figure 4. Overview of BrS genetic architecture in Thailand and European-ancestry populations.
Top, Graphical representation of the genetic contribution of rare and low-frequency variants to Brugada syndrome (BrS) in Thailand (**left**) and European ancestry populations (**right**), using a likely conservative estimate of a 4-fold higher prevalence of BrS in Thailand.[37,38] The absolute frequency of ultrarare loss-of-function coding variants in *SCN5A* is likely to be broadly similar in both ancestries (represented by the dark blue squares), but the diagnostic yield of such variants in BrS cohorts from Thailand is relatively lower (≈5% vs ≈20%) because of the different disease prevalence between ancestries (highlighted by the overall square sizes). A proportion of the additional susceptibility in Thai patients with BrS is explained by the low-frequency *SCN5A* coding variant p.Arg965Cys (≈6.5% of cases) and the noncoding RE5 enhancer variant described in this study (≈4% of cases). **Bottom**, Population frequencies of *SCN5A* p.Arg965Cys and RE5 variants in South and East Asian countries (see Table S8 for details of data sets used and exact variant frequencies; gray = data not available).

direct disruption of the *SCN5A* transcript by heterozygous nonsense or frameshift coding variants has been shown in numerous studies to lead to a maximum of 40% to 50% reduction in I_{Na} (using coexpression of wild-type and mutated proteins in electrophysiology assays to reflect the heterozygosity observed in patients): p.Glu473Ter,[39] p.Arg535Ter,[40] p.Trp822Ter,[41,42] p.Trp1191Ter,[43] and p.Leu1393Ter.[44] *SCN5A* variants affecting gene dosage (whether coding or noncoding) often have less deleterious effects than pathogenic *SCN5A* missense variants, which can exhibit dominant negative effects.[42]

The effect of rare regulatory variants at the *SCN5A* locus in individual patients is likely to be modified by the presence of risk or protective common variant haplotypes that have been identified in BrS GWAS. The complex genetic architecture of BrS at this and other genomic loci will at least partially explain the variable phenotypes observed in carriers of the RE5 variant, ranging from the highly symptomatic probands to the milder (or nonsymptomatic) phenotypes in relatives and the general Thai population database. The cumulative effect of these rare and common regulatory variants will ultimately determine the overall dosage of *SCN5A* across both alleles and, in conjunction with polygenic risk at other genomic loci, act to influence disease penetrance in individuals. Future precision medicine approaches will require not just a comprehensive assessment of overall genetic risk but an understanding of the allele-specific interaction between common and rare variation (eg, through the construction of haplotypes using long read genomic sequencing).

We observed a strong male predominance in the patients with BrS analyzed, both for the overall cohort (95%) and the RE5 variant carriers (100%; Table 1). The reflects a well-established sex bias for heritable cardiac diseases in general, and BrS in particular, which remains an incompletely understood phenomenon. Further research is required to

elucidate the factors underlying the large difference in sex-based penetrance in carriers of BrS pathogenic variants, and the implications this has for cascade screening and risk stratification in affected families.

The strong polygenic and common variant contributions to BrS highlighted by recent GWAS have revealed an increasingly complex genetic architecture for this condition.[5] This can lead to complicated inheritance patterns in affected families, as demonstrated in Figure 3A, where one of the individuals had a positive ajmaline test despite not carrying the RE5 variant. Such "nonsegregation" is not atypical in BrS family pedigrees; a previous study identified 8 noncarriers of familial rare *SCN5A* variants in 13 families who tested positive after ajmaline challenge, including in 2 families with truncating *SCN5A* variants of indisputable pathogenicity.[29] This complexity necessitates a nuanced approach to evaluating the pathogenicity of novel BrS-associated variants that encompasses genetic, computational, and functional lines of evidence.

This study highlights the potential of rare noncoding variation to account for some of the missing heritability in diseases such as BrS. The integrated approaches we describe here demonstrate the type of methods that can be applied to address the challenging task of characterizing noncoding pathogenic variants as we enter the era of routine genome sequencing. In particular, detailed epigenetic knowledge across disease-relevant genomic loci and the judicious use of computational evidence can help reduce the search space of the vast noncoding genome and identify putative variants of interest for functional validation. The identification of such novel pathogenic variant classes also benefits from expanding research to historically understudied populations, where founder variants can be readily identified in case–control studies, especially where diseases under investigation are more prevalent (such as BrS in Southeast Asia).

The persistence of at least 2 recurrent *SCN5A* loss-of-function variants of intermediate to large effect size in the Thai population (the RE5 variant and the *SCN5A*:p.Arg965Cys intermediate effect variant) is intriguing given their association with sudden death as BrS risk factors. Whereas selective pressure against pathogenic BrS variants may be relatively modest, as sudden death usually occurs in fourth or fifth decade, these variants (and likely other such risk factors in East Asian populations) appear to be restricted to this region. Several examples of disease risk factors that are protective against infectious diseases are known, such as the relationship between malaria and sickle cell trait or *APOL1* polymorphisms that protect against African sleeping sickness but increase the risk for chronic kidney disease.[45] Whether genetic variants associated with partially reduced sodium channel function confer similar protection is unknown, but would offer an intriguing hypothesis for the highly increased prevalence of BrS across Southeast Asia.

There are some limitations to this study. Whereas the genetic and functional data validate the pathogenicity of the RE5 variant and its role as the primary causal variant in these patients, the genetic architecture of BrS is complex. Additional common (and possibly rare) variant risk factors are likely to be contributing to the phenotype in the described cases, explaining the severity of the observed phenotypes. At the *SCN5A/SCN10A* locus, interaction between rare and common risk factors may determine the extent of reduced *SCN5A* expression and I_{Na}, which will require complex analysis and experimentation to resolve. Larger population genomics data sets will also be required to more precisely define the OR for the variant and determine whether it is also a risk factor in other Southeast Asian countries.

We have identified a rare, noncoding regulatory variant of large effect size at the *SCN5A* locus that is a major contributor to BrS risk in the Thai population. Improved knowledge of the genetic basis of arrhythmogenic diseases such as BrS offers the opportunity for proactively identifying and monitoring at-risk individuals to reduce the burden of sudden cardiac death, especially in Southeast Asia, where BrS is particularly prevalent. The inclusion of the RE5 variant in clinical genetic testing assays for BrS in Thailand may increase the diagnostic yield by one third (Figure 4). This will enable the identification and diagnosis of at-risk individuals in affected families allowing for targeted clinical monitoring and potentially treatment.[46] Based on the variant frequency in the Genomics Thailand database, we estimate that there are ≈43 000 carriers of the RE5 variant alone in Thailand. As genome sequencing becomes integrated into routine medical practice, the identification of variant carriers will enable more accurate assessment of its penetrance in the population and the initiation of clinical intervention, where appropriate, to prevent sudden cardiac death.

ARTICLE INFORMATION

Received February 14, 2024; accepted September 11, 2024.

Affiliations

Departments of Experimental Cardiology (R.W., I.M., F.M.B., A.O.V., M.K., L.B., C.R.B.) and Medical Biology (A.O.V., K.v.D., V.M.C.), Amsterdam University Medical Centers, University of Amsterdam, the Netherlands. Amsterdam Cardiovascular Sciences, Heart Failure and Arrhythmias, the Netherlands (R.W., I.M., F.M.B., A.O.V., A.S.A., K.V.V.L., P.G.P., M.K., L.B., V.M.C., A.A.M.W., C.R.B.). Member of the European Reference Network for Rare, Low Prevalence and Complex Diseases of the Heart: ERN GUARD-Heart (R.W., I.M., F.M.B., A.O.V., A.S.A., K.V.V.L., P.G.P., M.K., L.B., J.-J.S., R.R., J.B., A.A.M.W., C.R.B.). Department of Medicine, Center of Excellence in Arrhythmia Research (J.M., W.W., B.S., P.W., N.C., R.C., S.P., K.N., A.K.), and Departments of Pediatrics (Y.P., A.K.) and Forensic Medicine (K.V.) and Center of Excellence in Forensic Genetics, Ratchadapiseksompotch Fund (K.V., P.D.), Faculty of Medicine, Chulalongkorn University, Bangkok, Thailand. Department of Medicine, Piyavate Hospital, Bangkok, Thailand (N.C.). Forensic Serology and DNA, King Chulalongkorn Memorial Hospital and Thai Red Cross Society, Bangkok, Thailand (P.D.). Heart Rhythm Center, Division of Cardiology, Department of Medicine, Taipei Veterans General Hospital, Taiwan (C.-I.W.). Department of Medicine, Cardiovascular Genetics Center, Montreal Heart Institute and Faculty of Medicine, Université de Montréal, Quebec, Canada (R.T.). Department of Clinical Cardiology, Heart Centre, Amsterdam University Medical Centre, location AMC, the Netherlands (A.S.A., K.V.V.L., P.G.P., A.A.M.W.). Department of Medicine, Faculty of Medicine, Khon Kaen University, Thailand (D.S., P.M.). Departments of Medicine, Faculty of Medicine at Ramathibodi Hospital (M.A., T. Ngarmukos)

and Faculty of Medicine at Siriraj Hospital (R.K.), Mahidol University, Bangkok, Thailand. Department of Cardiovascular and Intervention, Central Chest Institute of Thailand, Nonthaburi, Thailand (A.A.). Department of Medicine, Maharat Nakhon Ratchasima Hospital, Nakorn Ratchasima, Thailand (K.P.). Bangkok Heart Hospital, Bangkok General Hospital, Thailand (G.V., A.K.). Illumina Cambridge Ltd, Granta Park, Great Abington, Cambridge, UK (Z.K., T. Newington, U.M., M.T.R.). Department of Biochemistry, University of Cambridge, UK (A.G.). Cardiology, Medicine, Barts Heart Centre, London, UK (P.D.L.). Institute of Cardiovascular Science, Population Health, UCL, London, UK (P.D.L.). Molecular and Clinical Sciences Research Institute, St. George's, University of London, UK (E.R.B.). Cardiology Clinical Academic Group, St. George's University Hospitals NHS Foundation Trust, London, UK (E.R.B.). Nantes Université, CHU Nantes, CNRS, INSERM, l'Institut du Thorax, Nantes, France (J.-J.S., R.R., J.B.). Pacific Rim Electrophysiology Research Institute, Bumrungrad Hospital, Bangkok, Thailand (K.N.).

Acknowledgments

The authors thank the National Biobank of Thailand, National Science and Technology Development Agency, for their assistance in gathering variant population frequency from the Genomics Thailand preliminary data.

Sources of Funding

Dr Mauleekoonphairoj received support by the Second Century Fund (C2F), Chulalongkorn University. Drs Poovorawan, Nademanee, and Khongphatthanayothin received support from the National Research Council of Thailand. Dr Wu received support from the Yin Shu-Tien Foundation, Taipei Veterans General Hospital–National Yang-Ming University Excellent Physician Scientists Cultivation Program (grant 108-V-A-013). Dr Behr received support from the Robert Lancaster Memorial Fund and UKRI. Dr Christoffels received support from EIC Pathfinder Challenges (grant Nav1.5-CARED) and the Netherlands Organization for Scientific Research (grant OCENW.GROOT.2019.029). Dr Bezzina received support from the Dutch Heart Foundation (grant CVON PREDICT2), the Netherlands Organization for Scientific Research (VICI fellowship 016.150.610), Fondation Leducq (grant 17CVD02), and EIC Pathfinder Challenges (grant Nav1.5-CARED).

Disclosures

None.

Supplemental Material

Methods
Tables S1–S8
Figures S1–S6
References 47–61

REFERENCES

1. Behr ER, Ben-Haim Y, Ackerman MJ, Krahn AD, Wilde AAM. Brugada syndrome and reduced right ventricular outflow tract conduction reserve: a final common pathway? *Eur Heart J*. 2021;42:1073–1081. doi: 10.1093/eurheartj/ehaa1051
2. Walsh R, Lahrouchi N, Tadros R, Kyndt F, Glinge C, Postema PG, Amin AS, Nannenberg EA, Ware JS, Whiffin N, et al; Nantes Referral Center for inherited cardiac arrhythmia. Enhancing rare variant interpretation in inherited arrhythmias through quantitative analysis of consortium disease cohorts and population controls. *Genet Med*. 2021;23:47–58. doi: 10.1038/s41436-020-00946-5
3. Hosseini SM, Kim R, Udupa S, Costain G, Jobling R, Liston E, Jamal SM, Szybowska M, Morel CF, Bowdin S, et al; National Institutes of Health Clinical Genome Resource Consortium. Reappraisal of reported genes for sudden arrhythmic death. *Circulation*. 2018;138:1195–1205. doi: 10.1161/CIRCULATIONAHA.118.035070
4. Wilde AAM, Semsarian C, Márquez MF, Shamloo AS, Ackerman MJ, Ashley EA, Sternick EB, Barajas-Martinez H, Behr ER, Bezzina CR, et al; Document Reviewers. European Heart Rhythm Association (EHRA)/Heart Rhythm Society (HRS)/Asia Pacific Heart Rhythm Society (APHRS)/Latin American Heart Rhythm Society (LAHRS) expert consensus statement on the state of genetic testing for cardiac diseases. *Europace*. 2022;24:1307–1367. doi: 10.1093/europace/euac030
5. Barc J, Tadros R, Glinge C, Chiang DY, Jouni M, Simonet F, Jurgens SJ, Baudic M, Nicastro M, Potet F, et al; KORA-Study Group. Genome-wide association analyses identify new Brugada syndrome risk loci and highlight a new mechanism of sodium channel regulation in disease susceptibility. *Nat Genet*. 2022;54:232–239. doi: 10.1038/s41588-021-01007-6
6. Man JCK, Mohan RA, van den Boogaard M, Hilvering CRE, Jenkins C, Wakker V, Bianchi V, de Laat W, Barnett P, Boukens BJ, et al. An enhancer cluster controls gene activity and topology of the SCN5A-SCN10A locus in vivo. *Nat Commun*. 2019;10:4943.
7. van der Harst P, van Setten J, Verweij N, Vogler G, Franke L, Maurano MT, Wang X, Mateo Leach I, Eijgelsheim M, Sotoodehnia N, et al. 52 Genetic loci influencing myocardial mass. *J Am Coll Cardiol*. 2016;68:1435–1448. doi: 10.1016/j.jacc.2016.07.729
8. Man JCK, Bosada FM, Scholman KT, Offerhaus JA, Walsh R, van Duijvenboden K, van Eif VWW, Bezzina CR, Verkerk AO, Boukens BJ, et al. Variant intronic enhancer controls SCN10A–short expression and heart conduction. *Circulation*. 2021;144:229–242. doi: 10.1161/CIRCULATIONAHA.121.054083
9. Brugada P, Brugada J. Right bundle branch block, persistent ST segment elevation and sudden cardiac death: a distinct clinical and electrocardiographic syndrome: a multicenter report. *J Am Coll Cardiol*. 1992;20:1391–1396. doi: 10.1016/0735-1097(92)90253-j
10. Nademanee K, Veerakul G, Nimmannit S, Chaowakul V, Bhuripanyo K, Likittanasombat K, Tunsanga K, Kuasirikul S, Malasit P, Tansupasawadikul S, et al. Arrhythmogenic marker for the sudden unexplained death syndrome in Thai men. *Circulation*. 1997;96:2595–2600. doi: 10.1161/01.cir.96.8.2595
11. Veerakul G, Khongphatthanayothin A, Nademanee K. Brugada syndrome in Thailand: three decades of progress. *Heart Rhythm O2*. 2022;3:743–751. doi: 10.1016/j.hroo.2022.08.011
12. Makarawate P, Glinge C, Khongphatthanayothin A, Walsh R, Mauleekoonphairoj J, Amnueypol M, Prechawat S, Wongcharoen W, Krittayaphong R, Anannab A, et al. Common and rare susceptibility genetic variants predisposing to Brugada syndrome in Thailand. *Heart Rhythm*. 2020;17:2145–2153. doi: 10.1016/j.hrthm.2020.06.027
13. Priori SG, Wilde AA, Horie M, Cho Y, Behr ER, Berul C, Blom N, Brugada J, Chiang C-E, Huikuri H, et al. HRS/EHRA/APHRS expert consensus statement on the diagnosis and management of patients with inherited primary arrhythmia syndromes: document endorsed by HRS, EHRA, and APHRS in May 2013 and by ACCF, AHA, PACES, and AEPC in June 2013. *Heart Rhythm*. 2013;10:1932–1963. doi: 10.1016/j.hrthm.2013.05.014
14. Richards S, Aziz N, Bale S, Bick D, Das S, Gastier-Foster J, Grody WW, Hegde M, Lyon E, Spector E, et al; ACMG Laboratory Quality Assurance Committee. Standards and guidelines for the interpretation of sequence variants: a joint consensus recommendation of the American College of Medical Genetics and Genomics and the Association for Molecular Pathology. *Genet Med*. 2015;17:405–424. doi: 10.1038/gim.2015.30
15. Moyon L, Berthelot C, Louis A, Nguyen NTT, Roest Crollius H. Classification of non-coding variants with high pathogenic impact. *PLoS Genet*. 2022;18:e1010191. doi: 10.1371/journal.pgen.1010191
16. Wu D, Dou J, Chai X, Bellis C, Wilm A, Shih CC, Soon WWJ, Bertin N, Lin CB, Khor CC, et al; SG10K Consortium. Large-scale whole-genome sequencing of three diverse Asian populations in Singapore. *Cell*. 2019;179:736–749.e15. doi: 10.1016/j.cell.2019.09.019
17. Tadaka S, Hishinuma E, Komaki S, Motoike IN, Kawashima J, Saigusa D, Inoue J, Takayama J, Okamura Y, Aoki Y, et al. jMorp updates in 2020: large enhancement of multi-omics data resources on the general Japanese population. *Nucleic Acids Res*. 2021;49:D536–D544. doi: 10.1093/nar/gkaa1034
18. Lee J, Lee J, Jeon S, Lee J, Jang I, Yang JO, Park S, Lee B, Choi J, Choi B-O, et al. A database of 5305 healthy Korean individuals reveals genetic and clinical implications for an East Asian population. *Exp Mol Med*. 2022;54:1862–1871. doi: 10.1038/s12276-022-00871-4
19. Heinz S, Benner C, Spann N, Bertolino E, Lin YC, Laslo P, Cheng JX, Murre C, Singh H, Glass CK. Simple combinations of lineage-determining transcription factors prime cis-regulatory elements required for macrophage and B cell identities. *Mol Cell*. 2010;38:576–589. doi: 10.1016/j.molcel.2010.05.004
20. Castro-Mondragon JA, Riudavets-Puig R, Rauluseviciute I, Lemma RB, Turchi L, Blanc-Mathieu R, Lucas J, Boddie P, Khan A, Manosalva Pérez N, et al. JASPAR 2022: the 9th release of the open-access database of transcription factor binding profiles. *Nucleic Acids Res*. 2022;50:D165–D173. doi: 10.1093/nar/gkab1113
21. Maas RGC, Lee S, Harakalova M, Snijders Blok CJB, Goodyer WR, Hjortnaes J, Doevendans PAFM, Van Laake LW, van der Velden J, Asselbergs FW, et al. Massive expansion and cryopreservation of functional human induced pluripotent stem cell-derived cardiomyocytes. *STAR Protoc*. 2021;2:100334. 10.1016/j.xpro.2021.100334
22. Dobin A, Davis CA, Schlesinger F, Drenkow J, Zaleski C, Jha S, Batut P, Chaisson M, Gingeras TR. STAR: ultrafast universal RNA-seq aligner. *Bioinformatics*. 2013;29:15–21. doi: 10.1093/bioinformatics/bts635
23. Koboldt DC, Zhang Q, Larson DE, Shen D, McLellan MD, Lin L, Miller CA, Mardis ER, Ding L, Wilson RK. VarScan 2: somatic mutation and copy number alteration discovery in cancer by exome sequencing. *Genome Res*. 2012;22:568–576. doi: 10.1101/gr.129684.111

24. Ruijter JM, Van Kampen AHC, Baas F. Statistical evaluation of SAGE libraries: consequences for experimental design. *Physiol Genomics*. 2002;11:37–44. doi: 10.1152/physiolgenomics.00042.2002
25. Ten Hoope W, Hollmann MW, de Bruin K, Verberne HJ, Verkerk AO, Tan HL, Verhamme C, Horn J, Rigaud M, Picardi S, et al. Pharmacodynamics and pharmacokinetics of lidocaine in a rodent model of diabetic neuropathy. *Anesthesiology*. 2018;128:609–619. doi: 10.1097/ALN.0000000000002035
26. Veerman CC, Mengarelli I, Guan K, Stauske M, Barc J, Tan HL, Wilde AAM, Verkerk AO, Bezzina CR. hiPSC-derived cardiomyocytes from Brugada Syndrome patients without identified mutations do not exhibit clear cellular electrophysiological abnormalities. *Sci Rep*. 2016;6:30967. doi: 10.1038/srep30967
27. Eroglu TE, Mohr GH, Blom MT, Verkerk AO, Souverein PC, Torp-Pedersen C, Folke F, Wissenberg M, van den Brink L, Davis RP, et al. Differential effects on out-of-hospital cardiac arrest of dihydropyridines: real-world data from population-based cohorts across two European countries. *Eur Heart J Cardiovasc Pharmacother*. 2020;6:347–355. doi: 10.1093/ehjcvp/pvz038
28. Wilde AAM, Amin AS, Morita H, Tadros R. Use, misuse, and pitfalls of the drug challenge test in the diagnosis of the Brugada syndrome. *Eur Heart J*. 2023;44:2427–2439. doi: 10.1093/eurheartj/ehad295
29. Probst V, Wilde AAM, Barc J, Sacher F, Babuty D, Mabo P, Mansourati J, Le Scouarnec S, Kyndt F, Le Caignec C, et al. SCN5A mutations and the role of genetic background in the pathophysiology of Brugada syndrome. *Circ Cardiovasc Genet*. 2009;2:552–557. doi: 10.1161/CIRCGENETICS.109.853374
30. Nademanee K, Hocini M, Haïssaguerre M. Epicardial substrate ablation for Brugada syndrome. *Heart Rhythm*. 2017;14:457–461. doi: 10.1016/j.hrthm.2016.12.001
31. Ciconte G, Monasky MM, Santinelli V, Micaglio E, Vicedomini G, Anastasia L, Negro G, Borrelli V, Giannelli L, Santini F, et al. Brugada syndrome genetics is associated with phenotype severity. *Eur Heart J*. 2021;42:1082–1090. doi: 10.1093/eurheartj/ehaa942
32. Visel A, Minovitsky S, Dubchak I, Pennacchio LA. VISTA Enhancer Browser: a database of tissue-specific human enhancers. *Nucleic Acids Res*. 2007;35:D88–D92. doi: 10.1093/nar/gkl822
33. Dantas Machado AC, Cooper BH, Lei X, Di Felice R, Chen L, Rohs R. Landscape of DNA binding signatures of myocyte enhancer factor-2B reveals a unique interplay of base and shape readout. *Nucleic Acids Res*. 2020;48:8529–8544. doi: 10.1093/nar/gkaa642
34. Akerberg BN, Gu F, VanDusen NJ, Zhang X, Dong R, Li K, Zhang B, Zhou B, Sethi I, Ma Q, et al. A reference map of murine cardiac transcription factor chromatin occupancy identifies dynamic and conserved enhancers. *Nat Commun*. 2019;10:4907. doi: 10.1038/s41467-019-12812-3
35. Anguita E, Candel FJ, Chaparro A, Roldán-Etcheverry JJ. Transcription factor GFI1B in health and disease. *Front Oncol*. 2017;7:54. doi: 10.3389/fonc.2017.00054
36. Berecki G, Wilders R, de Jonge B, van Ginneken ACG, Verkerk AO. Re-evaluation of the action potential upstroke velocity as a measure of the Na+ current in cardiac myocytes at physiological conditions. *PLoS One*. 2010;5:e15772. doi: 10.1371/journal.pone.0015772
37. Vutthikraivit W, Rattanawong P, Putthapiban P, Sukhumthammarat W, Vathesatogkit P, Ngarmukos T, Thakkinstian A. Worldwide prevalence of Brugada syndrome: a systematic review and meta-analysis. *Acta Cardiol Sin*. 2018;34:267–277. doi: 10.6515/ACS.201805_34(3).20180302B
38. Marsman EMJ, Postema PG, Remme CA. Brugada syndrome: update and future perspectives. *Heart*. 2022;108:668–675. doi: 10.1136/heartjnl-2020-318258
39. Baroudi G, Napolitano C, Priori SG, Del Bufalo A, Chahine M. Loss of function associated with novel mutations of the SCN5A gene in patients with Brugada syndrome. *Can J Cardiol*. 2004;20:425–430.
40. Keller DI, Rougier J-S, Kucera JP, Benammar N, Fressart V, Guicheney P, Madle A, Fromer M, Schläpfer J, Abriel H. Brugada syndrome and fever: genetic and molecular characterization of patients carrying SCN5A mutations. *Cardiovasc Res*. 2005;67:510–519. doi: 10.1016/j.cardiores.2005.03.024
41. Keller DI, Barrane F-Z, Gouas L, Martin J, Pilote S, Suarez V, Osswald S, Brink M, Guicheney P, Schwick N, et al. A novel nonsense mutation in the SCN5A gene leads to Brugada syndrome and a silent gene mutation carrier state. *Can J Cardiol*. 2005;21:925–931.
42. O'Neill MJ, Muhammad A, Li B, Wada Y, Hall L, Solus JF, Short L, Roden DM, Glazer AM. Dominant negative effects of SCN5A missense variants. *Genet Med*. 2022;24:1238–1248. doi: 10.1016/j.gim.2022.02.010
43. Shin D-J, Kim E, Park S-B, Jang W-C, Bae Y, Han J, Jang Y, Joung B, Lee MH, Kim SS, et al. A novel mutation in the SCN5A gene is associated with Brugada syndrome. *Life Sci*. 2007;80:716–724. doi: 10.1016/j.lfs.2006.10.025
44. Samani K, Ai T, Towbin JA, Brugada R, Shuraih M, Xi Y, Wu G, Cheng J, Vatta M. A nonsense SCN5A mutation associated with Brugada-type electrocardiogram and intraventricular conduction defects. *Pacing Clin Electrophysiol*. 2009;32:1231–1236. doi: 10.1111/j.1540-8159.2009.02470.x
45. Genovese G, Friedman DJ, Ross MD, Lecordier L, Uzureau P, Freedman BI, Bowden DW, Langefeld CD, Oleksyk TK, Uscinski Knob AL, et al. Association of trypanolytic ApoL1 variants with kidney disease in African Americans. *Science*. 2010;329:841–845. doi: 10.1126/science.1193032
46. Nademanee K, Chung F-P, Sacher F, Nogami A, Nakagawa H, Jiang C, Hocini M, Behr E, Veerakul G, Jan Smit J, et al. Long-term outcomes of Brugada substrate ablation: a report from BRAVO (Brugada Ablation of VF Substrate Ongoing Multicenter Registry). *Circulation*. 2023;147:1568–1578. doi: 10.1161/CIRCULATIONAHA.122.063367
47. Li H, Durbin R. Fast and accurate short read alignment with Burrows-Wheeler transform. *Bioinformatics*. 2009;25:1754–1760. doi: 10.1093/bioinformatics/btp324
48. Danecek P, Bonfield JK, Liddle J, Marshall J, Ohan V, Pollard MO, Whitwham A, Keane T, McCarthy SA, Davies RM, et al. Twelve years of SAMtools and BCFtools. *GigaScience*. 2021;10:giab008. 10.1093/gigascience/giab008
49. Tarasov A, Vilella AJ, Cuppen E, Nijman IJ, Prins P. Sambamba: fast processing of NGS alignment formats. *Bioinformatics*. 2015;31:2032–2034. doi: 10.1093/bioinformatics/btv098
50. Poplin R, Ruano-Rubio V, DePristo MA, Fennell TJ, Carneiro MO, Van der Auwera GA, Kling DE, Gauthier LD, Levy-Moonshine A, Roazen D, et al. Scaling accurate genetic variant discovery to tens of thousands of samples. *bioRxiv*. Preprint posted July 24, 2018. doi: 10.1101/201178
51. Mölder F, Jablonski KP, Letcher B, Hall MB, Tomkins-Tinch CH, Sochat V, Forster J, Lee S, Twardziok SO, Kanitz A, et al. Sustainable data analysis with Snakemake. *F1000Research*. 2021;10:33. doi: 10.12688/f1000research.29032.2
52. Tohyama S, Hattori F, Sano M, Hishiki T, Nagahata Y, Matsuura T, Hashimoto H, Suzuki T, Yamashita H, Satoh Y, et al. Distinct metabolic flow enables large-scale purification of mouse and human pluripotent stem cell-derived cardiomyocytes. *Cell Stem Cell*. 2013;12:127–137. doi: 10.1016/j.stem.2012.09.013
53. Verkerk AO, Doszpod IJ, Mengarelli I, Magyar T, Polyák A, Pászti B, Efimov IR, Wilders R, Koncz I. Acetylcholine reduces L-type calcium current without major changes in repolarization of canine and human Purkinje and ventricular tissue. *Biomedicines*. 2022;10:2987. doi: 10.3390/biomedicines10112987
54. Creemers EE, Sutherland LB, Oh J, Barbosa AC, Olson EN. Coactivation of MEF2 by the SAP domain proteins myocardin and MASTR. *Mol Cell*. 2006;23:83–96. doi: 10.1016/j.molcel.2006.05.026
55. Nasilli G, Yiangou L, Palandri C, Cerbai E, Davis RP, Verkerk AO, Casini S, Remme CA. Beneficial effects of chronic mexiletine treatment in a human model of SCN5A overlap syndrome. *Europace*. 2023;25:euad154. doi: 10.1093/europace/euad154
56. Campostrini G, Kosmidis G, Ward-van Oostwaard D, Davis RP, Yiangou L, Ottaviani D, Veerman CC, Mei H, Orlova VV, Wilde AAM, et al. Maturation of hiPSC-derived cardiomyocytes promotes adult alternative splicing of SCN5A and reveals changes in sodium current associated with cardiac arrhythmia. *Cardiovasc Res*. 2023;119:167–182. 10.1093/cvr/cvac059
57. Marchal GA, Jouni M, Chiang DY, Pérez-Hernández M, Podliesna S, Yu N, Casini S, Potet F, Veerman CC, Klerk M, et al. Targeting the microtubule EB1-CLASP2 complex modulates NaV1.5 at intercalated discs. *Circ Res*. 2021;129:349–365. doi: 10.1161/CIRCRESAHA.120.318643
58. Casini S, Marchal GA, Kawasaki M, Nariswari FA, Portero V, van den Berg NWE, Guan K, Driessen AHG, Veldkamp MW, Mengarelli I, et al. Absence of functional Nav1.8 channels in non-diseased atrial and ventricular cardiomyocytes. *Cardiovasc Drugs Ther*. 2019;33:649–660. doi: 10.1007/s10557-019-06925-6
59. Ma D, Liu Z, Loh LJ, Zhao Y, Li G, Liew R, Islam O, Wu J, Chung YY, Teo WS, et al. Identification of an INa-dependent and Ito-mediated proarrhythmic mechanism in cardiomyocytes derived from pluripotent stem cells of a Brugada syndrome patient. *Sci Rep*. 2018;8:11246. doi: 10.1038/s41598-018-29574-5
60. Veerman CC, Mengarelli I, Lodder EM, Kosmidis G, Bellin M, Zhang M, Dittmann S, Guan K, Wilde AAM, Schulze-Bahr E, et al. Switch from fetal to adult SCN5A isoform in human induced pluripotent stem cell-derived cardiomyocytes unmasks the cellular phenotype of a conduction disease-causing mutation. *J Am Heart Assoc*. 2017;6:e005135. doi: 10.1161/JAHA.116.005135
61. Portero V, Casini S, Hoekstra M, Verkerk AO, Mengarelli I, Belardinelli L, Rajamani S, Wilde AAM, Bezzina CR, Veldkamp MW, et al. Anti-arrhythmic potential of the late sodium current inhibitor GS-458967 in murine Scn5a-1798insD± and human SCN5A-1795insD± iPSC-derived cardiomyocytes. *Cardiovasc Res*. 2017;113:829–838. doi: 10.1093/cvr/cvx077